

M. KOPERNIK<sup>\*,#</sup>, A. MILENIN<sup>\*</sup>, S. KAĆ<sup>\*</sup>

## NUMERICAL AND EXPERIMENTAL ANALYSIS OF FRACTURE OF ATHROMBOGENIC COATINGS DEPOSITED ON VENTRICULAR ASSIST DEVICE IN MICRO-SHEAR TEST

### NUMERYCZNA I DOŚWIADCZALNA ANALIZA PĘKANIA ATROMBOGENNYCH POWŁOK NANOSZONYCH NA KOMORY WSPOMAGANIA PRACY SERCA W PRÓBIE MIKROŚCINANIA

The Polish left ventricular assist device (LVAD – RELIGA\_EXT) will be made of thermoplastic polycarbonate-urethane (Bionate II) with deposited athrombogenic nano-coatings: gold (Au) and titanium nitride (TiN). Referring to the physical model, the two-scale model of LVAD developed in the previous works in the authors' finite element code is composed of a macro-model of blood chamber and a micro-model of wall: TiN, Au and Bionate II. The numerical analysis of stress and strain states confirmed the possibility of fracture based on localization of zones of the biggest values of triaxiality factor. The introduction of Au interlayer between TiN and polymer improved the toughness of the connection, and increased the compressive residual stress in the coating what resulted in reduction of stress and strain close to the boundary between substrate and coating.

However, the proper design of multilayer wall of the medical device requires the introduction of the real stress and strain states in the deposited coatings. The characteristics of TiN nano-coating such as residual stress, material model and fracture model were determined in the previously completed studies such as experimental and numerical nanoindentation tests, profilometry studies and *in situ* SEM's micro-tension tests.

The experimental *in situ* SEM's micro-shear test was performed in the present paper and the corresponding numerical model of the test was also developed, and then, interpreted. The critical strains taken from experiment and considered as the effective strains in the model of test are the values which are the function of triaxiality factors for the tested samples. The developed in the authors' FE code model of multilayer wall of VAD enriched with critical strain determined in the present paper enables prediction of fracture.

**Keywords:** micro-shear test, finite element method (FEM), fracture, ventricular assist device (VAD), titanium nitride (TiN), gold (Au)

Polska lewa komora wspomaganie pracy serca (LVAD – RELIGA\_EXT) zostanie wykonana z termoplastycznego poliwęglano-uretanu (Bionate II) z naniesionymi atrombogenicznymi powłokami: złota (Au) i azotku tytanu (TiN). W odniesieniu do modelu fizycznego, dwuskalowy model komory LVAD opracowany we wcześniejszych pracach w autorskim kodzie elementów skończonych jest złożony z modelu makro czaszy krwistej i z mikro-modelu ściany: TiN, Au i Bionate II. Analiza numeryczna stanów naprężenia i odkształcenia potwierdziła prawdopodobieństwo pęknięcia poprzez zlokalizowanie stref o największej wartości współczynnika naprężenia trójosiowego. Wprowadzenie międzywarstwy złota pomiędzy TiN i polimer poprawiło wytrzymałość tego połączenia i powiększyło ściskające naprężenie własne w powłoce, co doprowadziło do redukcji naprężenia i odkształcenia blisko granicy pomiędzy podłożem i powłoką.

Jednakże, właściwy projekt wielowarstwowej ściany urządzenia medycznego wymaga wprowadzenia rzeczywistych stanów naprężeń i odkształceń w naniesionych powłokach. Charakterystyki powłok TiN takie jak naprężenie własne, model materiału i model pęknięcia zostały określone we wcześniej wykonanych badaniach takich jak doświadczalne i numeryczne testy nanoindentacji, badania profilometryczne, i testy mikrorozciągania prowadzone pod elektronowym mikroskopem skaningowym.

W niniejszej pracy przeprowadzono doświadczalny test mikrościnnania pod skaningowym mikroskopem elektronowym, opracowano model numeryczny tego testu, a następnie go zinterpretowano. Odkształcenia krytyczne otrzymane z doświadczenia i określone w modelu testu jako intensywność odkształcenia są wartościami będącymi funkcją współczynników naprężeń trójosiowych dla badanych próbek. Opracowany w kodzie własnym model elementów skończonych wielowarstwowej ściany komory VAD wzbogacony o określone w niniejszej pracy odkształcenia krytyczne umożliwia przewidywanie pęknięcia.

### 1. Introduction

The main advantage of simple shear test [1] is achievement of large deformation without plastic instability in com-

parison with the uniaxial tensile test or the plane strain tensile test. Theoretical and experimental studies showed that stress triaxiality [2] is the key parameter controlling the magnitude of the fracture strain in mechanical tests. There is a mount-

\* AGH UNIVERSITY OF SCIENCE AND TECHNOLOGY, AL. A. MICKIEWICZA 30, 30-059 KRAKÓW, POLAND

# Corresponding author: kopernik@agh.edu.pl

ing evidence [3] that the normalized third deviatoric stress invariant (equivalent to the Lode's angle parameter) should also be included in characterization of ductile fracture. Therefore, the damage models applied in finite element models of shear tests should be composed of the stress triaxiality and the Lode's angle parameter. The comparisons of damage models based on the introduced key parameters was done for the Gurson-Tvergaard-Needleman's model in [4] and for the Lemaitre and Wierzbicki-Xue' model in [5]. The evaluation, calibration and validation of the damage models implemented in finite element shear tests is often carried out in experimental pure tensile conditions [4], digital image correlation tests [5] and in micro-double shear test coupled with simultaneous nanoindentation test [6].

Several parameters have influence on results of micro-shear tests. The effect of specimen geometry, the edge effect based on specimen geometry and material parameters on work hardening, and distribution of shear strain were investigated in experimental and finite element shear tests in [7]. Considering the presented key parameters of damage models, there is also strong relation between specimen's geometry and initial level of stress triaxiality what is shown in [4]. Another parameters associated with the sample are sample's constraints which have influence on character of micro-shear cracks in [8].

The damage models based on key parameters (stress triaxiality and Lode's angle parameter) are the most commonly used for finite element modeling of shear fracture of steels and alloys in different forming processes, for example the modified Mohr-Coulomb fracture criterion was adopted to problems involving ductile fracture of materials and sheets to predict shear fracture in [9]. The results of shear tests are also applied in the multi-scale models as an input data, for example the multi-scale

hierarchical constitutive model was developed in [10] for establishing the relationship between quantum mechanical, micro-mechanical, and overall strength/toughness properties in steel design.

The similar approach to application of results of micro-shear tests is proposed in the present paper. The two-scale model [11] of Polish ventricular assist device [12,13] developed in the authors' finite element code was composed of a macro- model of blood chamber [14] and a micro-model [15] of wall: TiN and Bionate II (thermoplastic polycarbonate-urethane). The numerical analysis of stress and strain states [16] confirmed the possibility of fracture [17] based on localization of zones of the biggest values of triaxiality factor. The introduction of Au interlayer between TiN and polymer suggested in [18] changes a stress state in the material system. The Au interlayer helps to improve toughness of the connection and to increase the compressive residual stress in the coating what results in reduction of stress and strain close to the boundary between substrate and coating. Thus, the suggested composition of materials of wall of VAD (ventricular assist device) is enriched with Au nano-coating in the present work.

The proper design of multilayer wall of the medical device [19] requires the introduction of the real stress and strain states in the deposited coatings. The mechanical properties of TiN nano-coating such as residual stress, material model and fracture model were determined in experimental and numer-

cial nanoindentation tests [20], profilometry studies [18] and *in situ* SEM's (scanning electron microscopy) micro-tension tests [17].

The goal of present work is development of the experimental *in situ* SEM's micro-shear test, the numerical model of the test, and then, its interpretation. The critical strains taken from experiment and considered as the effective strains in the model of test are the values which are the function of triaxiality factors for the tested samples. The FE model of multilayer wall of VAD enriched with critical strain enables prediction of fracture. We hope that proposed approach will be helpful to enrich the knowledge of the optimal structure of the VAD and moreover, provide methodology for development of similar structures dedicated for other applications.

## 2. *In situ* SEM's micro-shear test and results

The TiN nano-coatings were deposited on the Bionate II substrates by using pulsed Nd:YAG laser system proposed at the WIMiP AGH [21]. The parameters of deposition process were: 100 mJ energy of laser beam, 266 nm wavelength, 4.2 J/cm<sup>2</sup> fluence, 25°C temperature of substrate, 12 ns pulse duration at a repetition rate of 10 Hz and 5000 laser shots. The gold nano-coatings of thickness 5 nm were deposited as interlayers between the TiN and Bionate II. The gold was deposited by a magnetron sputtering method with a discharge current 10 mA and a deposition time 5 min.

The verification of thicknesses of deposited coatings was done in AFM and TEM studies (Fig. 1). The detailed analysis

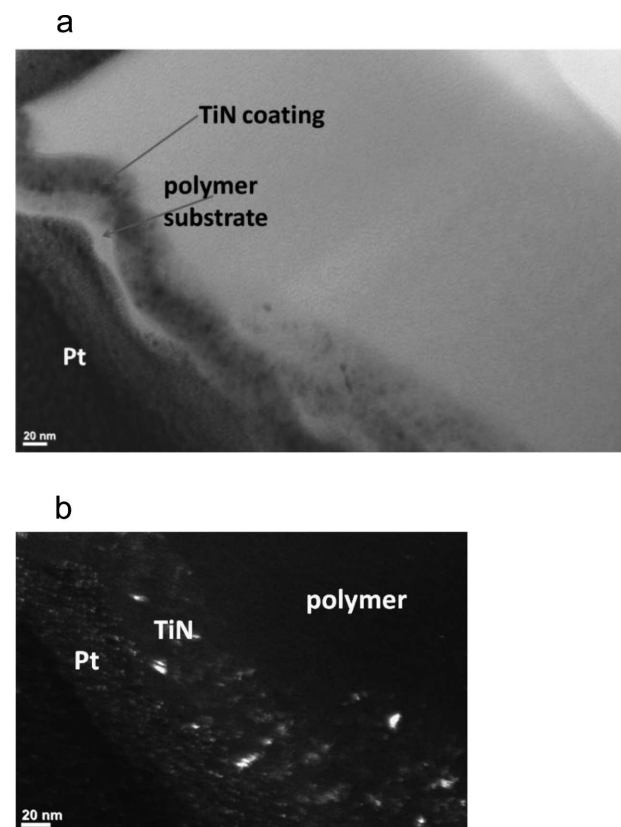


Fig. 1. a) The TEM's image of cross-section of the TiN coating deposited on Bionate II. b) The TEM's image of cross-section of the TiN coating deposited on Bionate II in dark field of view with visible crystallites

of micro-structure of TiN coating on polymer substrate was done on transmission electron microscope JEM-2010ARP produced by JEOL. The TiN coatings have thicknesses in the range of 30-35 nm. The electron diffraction analysis in the coating showed presence of a regular crystalline structure centered-cubic TiN phase. The crystallite diameter estimated from TEM's images taken in a dark field of view is less than 10 nm. The chemical composition analysis was performed by TEM-EDS and STEM-EDS.

The micro-shear test was performed directly during the Scanning Electron Microscope (SEM) observation. For this purpose, the Hitachi 3500-N SEM with Kammrath and Weiss GmbH 5kN tensile/compression module was applied. The shape of sample used in the *in situ* SEM's micro-shear test with marked area by hatched rectangle in the center of the sample is presented in Fig. 2. The average thickness of each of 10 specimens was 3 mm. The average measured distance between two points in the center of each specimen was 5 mm. The center part of each specimen was analysed under SEM in the micro-shear test. During shear tests the samples were elongated by steps, and tensile force in the range from 0 to 18 N and elongation from 0 to 1356  $\mu\text{m}$  were applied. After each step of elongation the surface of deformed thin film was observed using SEM (magnification from 35 to 12 000 x) in order to detect cracks appearance.

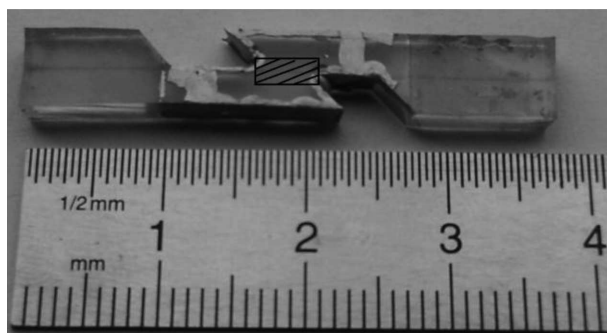


Fig. 2. The shape of sample used in the *in situ* SEM's micro-shear test with marked area by hatched rectangle in the center of the sample

The SEM's images taken for four of samples in *in situ* SEM's micro-shear test are shown on Figs.3-6. The conditions of appearance of the first cracks for four samples are presented in the TABLE 1. For the sample nr 1 the first cracks appeared around "inclusions" in the polyurethane under tension force of 6N (displacement of 212  $\mu\text{m}$ , Fig. 3a). However, the first cracks in the sample 1 from TABLE 1 which are not connected with "inclusions" are visible in the coating under tension force 7N (displacement of 252  $\mu\text{m}$ , Fig. 3b). The sample nr 2 had no visible "inclusions" in polyurethane, thus the first cracks were observed under tension force of 8 N (displacement of 110  $\mu\text{m}$ , Fig. 4). The similar observations were done for the sample nr 3, for which the first cracks were noticed under tension force 7 N (displacement of 137  $\mu\text{m}$ , Fig. 5a). The very large deformation, wear and chipping of the coating were registered under tension force 11 N for the sample nr 3 (displacement of 536  $\mu\text{m}$ , Fig. 5b). For the last of analysed samples (sample nr 4), the first cracks appeared under tension force 7 N (displacement of 164  $\mu\text{m}$ , Fig. 6a). However, for the last sample the bigger cracks appeared under tension force 8 N

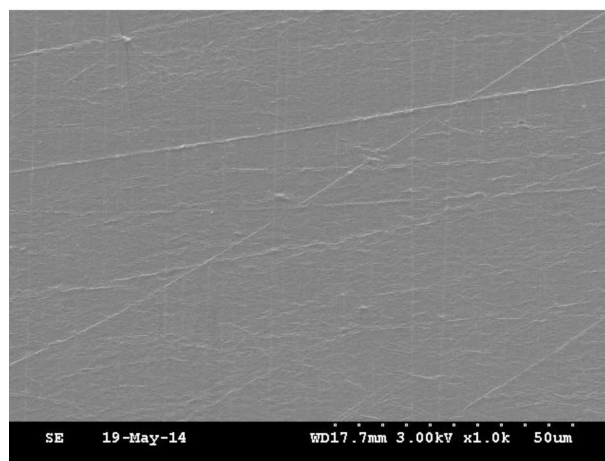
(displacement 184  $\mu\text{m}$ , Fig. 6b) in the corner of sample, near notch. For all of the samples the regions on the longer axis of the sample passing through its center were also investigated during the micro-shear test, but no cracks were observed.

TABLE 1

The conditions of appearance of the first cracks in the *in situ* SEM's micro-shear test for four selected samples

nr of sample	resolution	force, N	displacement, $\mu\text{m}$	distance between two points in the center of specimen, mm
1	1000 x	6	212	5.0
1	3000 x	7	252	5.0
2	300 x	8	110	4.5
3	150 x	7	137	6.5
3	150 x	11	536	6.5
4	500 x	7	164	4.5
4	35 x	8	184	4.5

a



b

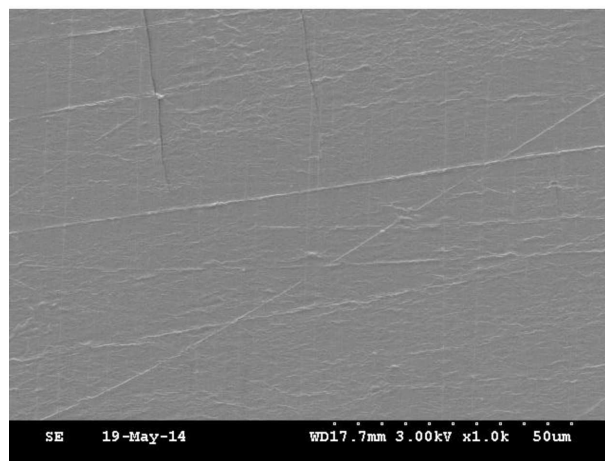


Fig. 3. a) The SEM's image of the first cracks around "inclusions" in the polyurethane in the micro-shear test for the sample nr 1 from Table 1 (force 6 N). b) The SEM's image of the first cracks in the micro-shear test for the sample nr 1 from Table 1 (force 7 N)



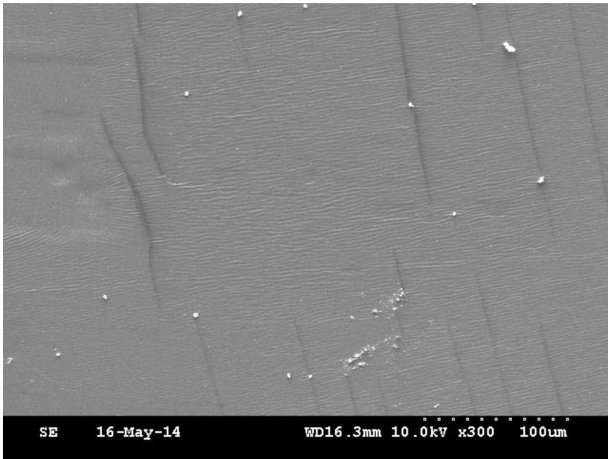


Fig. 4. The SEM's image of the first cracks in the micro-shear test for the sample nr 2 from Table 1 (force 8 N)

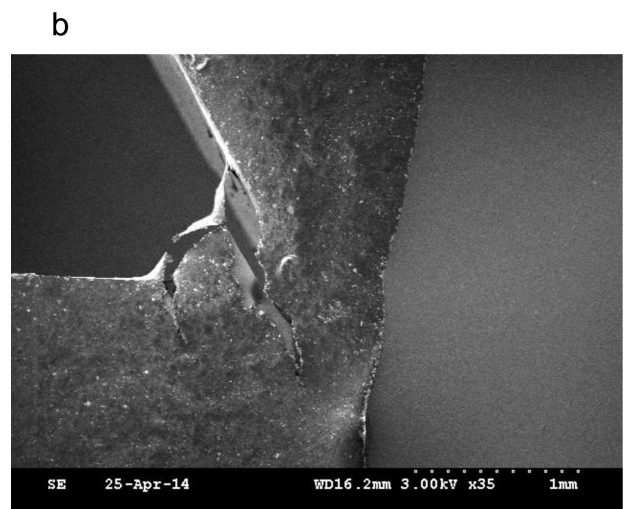
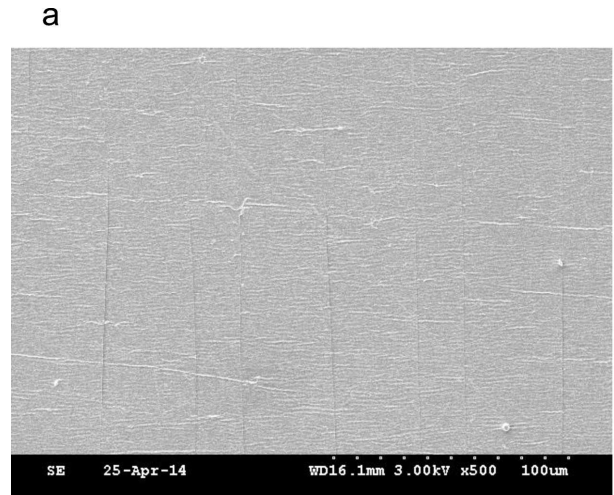


Fig. 6. a) The SEM's image of the first cracks in the micro-shear test for the sample nr 4 from Table 1 (force 7 N). b) The SEM's image of the big cracks in the micro-shear test for the sample nr 4 from Table 1 (force 8 N) in the corner of sample

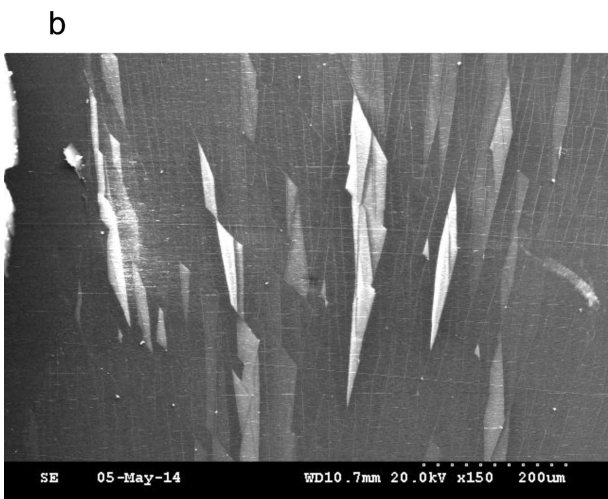
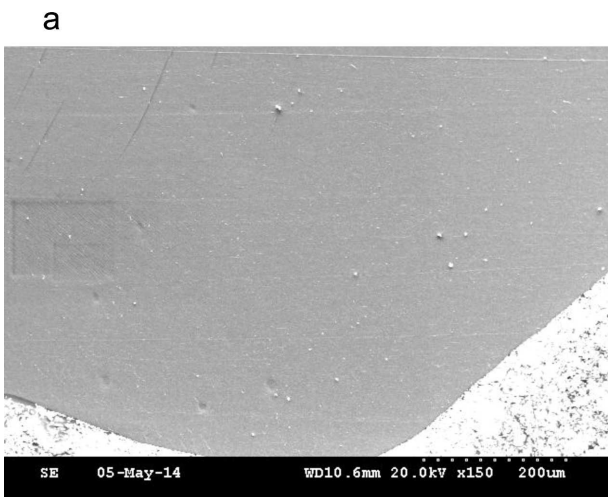


Fig. 5. a) The SEM's image of the first cracks in the micro-shear test for the sample nr 3 from Table 1 (force 7 N). b) The SEM's image of the big cracks in the micro-shear test for the sample nr 3 from Table 1 (force 11 N)

Behaviour of the coating during micro-shear test was modelled using the finite elements (FE) code. Methodology and selected results are presented in section 3.

### 3. Model of micro-shear test and results

The developed VADFEM computer program allows to model the strain-stress states in the multi-layer prototypes of ventricular assist devices [14]. The multi-scale model of VAD developed in the FE code [11,12] is composed of a macro-model of the blood chamber [16] and a micro-model of the VAD's wall [15] composed of the gold and TiN nano-coating deposited on polymer. The material models of TiN and polymer used in computations were identified in [12,20].

The macro-scale boundary problem is formulated by the theory of a non-linear elasticity and a distribution of displacements. The proposed approach describes deformation of the blood chamber of VAD under a blood pressure, if: a stress is related to a strain by a non-linear equations (according to the non-linear theory of elasticity) and a strain disappears in an unloading conditions. The non-linearity in an elastic deformation process of the blood chamber is a result of: a non-linear mechanical properties of the polymer and a non-linear mechanical properties of the TiN nano-coating. The problem of

the blood chamber deformation on a macro scale is considered as a 3D solution. Thus, the defined boundary problem of a theory of non-linear elasticity is composed of the groups of equations described in [22]. The Young's modulus is assumed as a constant value in a case of a small non-linearity of material. A tetrahedron finite element with a five-point scheme of integration is used in the macro-model of VAD. The average number of applied nodes is 50 000, and the average number of applied tetrahedron finite elements is 150 000. The boundary conditions applied in the macro-model of VAD are in accordance with settings of the physical experiment [12].

The FE macro-model of the VAD allows to distinguish a failure areas of the loaded model on the basis of a strain and a stress analysis. The triaxiality factor ( $k = 0.15$ ) in the FE macro-model was calculated in the failure areas which are located on the inner surface of blood chamber between two connectors (Fig.7a). The reached value of triaxiality factor ( $k = 0.15$ ) [9] indicates probability of a pure shear-induced-fracture.

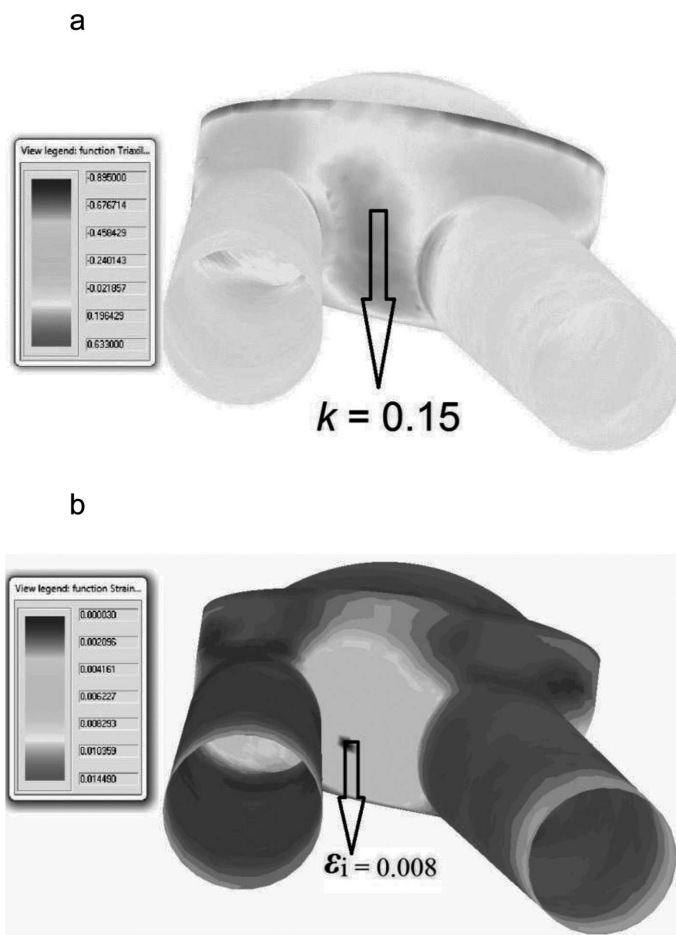


Fig. 7. The distributions of a) triaxiality factor, and b) effective strain in the FE model of blood chamber

Therefore, the micro-shear test was performed for the samples (section 2.1) composed of TiN, Au and polymer, and the corresponding FE model of micro-shear test was built for the system of materials of blood chamber. The non-linearity of mechanical properties of the TiN nano-coating and the polymer are observed. Thus, an elastic-plastic and a non-linear elastic material models, as well as their corresponding theories, are used in computations.

The micro-scale boundary problem is solved by the FE model composed of 16 200 three-dimensional hexahedral FEs and 43 600 nodes. Three layers of finite elements were applied in the model, one layer of finite elements was used for each material. The several densities of FE meshes were tested and the FE mesh shown in Figs. 8 and 9 was used in computations. The mechanical properties of the material system TiN/Au/Bionate II are assumed as following:

1. The bilinear, elastic-plastic material model of the TiN nano-coating is described by the parameters identified in [20]:  $\epsilon_1 = 0.009$ ,  $\sigma_1 = 2\,614$  MPa,  $\epsilon_2 = 0.166$  and  $\sigma_2 = 9\,107$  MPa, and the Poisson's ratio 0.25.
2. The Hollomon's material model of the Bionate II at a room temperature is identified in [17]:  $36.45\epsilon^{0.72}$  basing on results given by the Foundation of Cardiac Surgery Development in Poland, and the Poisson's ratio 0.4.
3. The properties of Au coating given in [23] are: the average Young's modulus 132.73 GPa and the Poisson's ratio 0.3.

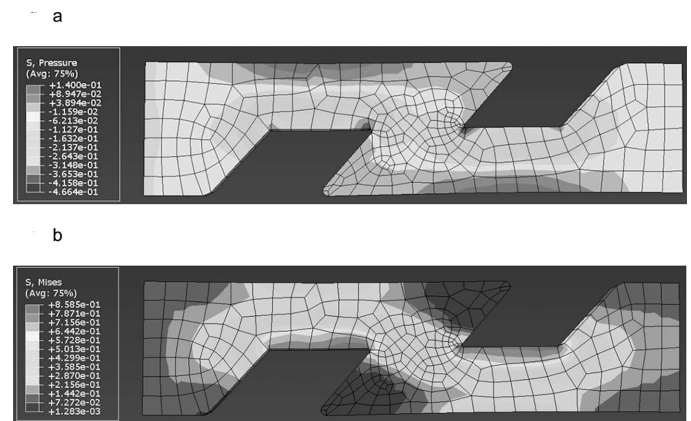


Fig. 8. The distributions of a) mean stress, and b) effective stress in the FE model of micro-shear test

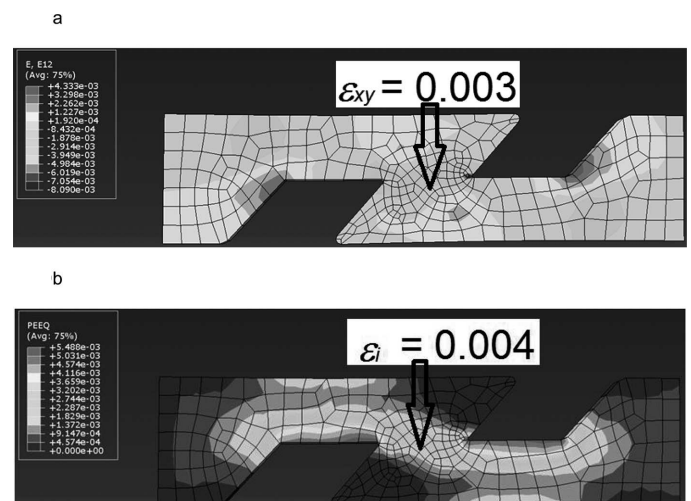


Fig. 9. The distributions of a) tangential strain and b) effective strain in the FE model of micro-shear test

The boundary conditions are taken from experiment and displacements are equal to values given in Table 1 for sample nr 2. The sample nr 2 was selected as the modelled sample, because fracture observed for the sample nr 2 captures the most representative cracking behavior of all of the tested

samples (compare Fig. 4). The triaxiality factor computed in the center of the sample is  $k = 0.15$  (Fig. 8) and it the same as the value reached in the failure areas of the model of blood chamber (Fig. 7a). The results of FE calculations as distributions of tangential strain and effective strain are showed in Fig. 9. In experiment and numerical model of micro-shear test the critical strain (effective strain) was determined in the TiN nano-coating and it is 0.004 (Fig.9 b). However, in the model of blood chamber for the same value of triaxiality factor the critical strain is 0.008 (Fig. 7b).

Therefore, in the model of blood chamber in region located between two connectors the probability of fracture is quite big, because the critical strain computed in the micro-model is reached. Basing on the introduced results, it is recommended not to deposit TiN coating in zones between two connectors of the blood chamber. The clots are not observed in experimental tests in the failure areas of blood chamber. Thus, the application of athrombogenic coatings in these regions is not necessary what is the main practical conclusion of the present work.

#### 4. Conclusions

**A.** The multi-scale FE model of left ventricular assist device was proposed for determination of the failure areas of TiN coating.

**B.** It was observed that under pressure loading of blood chamber set on its inner surface, the stress state in failure areas is different from linear. Therefore, the model of fracture of the TiN coating have to be designed around this stress state.

**C.** The physical simulation of the failure area of blood chamber was proposed for a micro-shear test of samples composed of TiN and Au nano-coatings deposited on polymer. The results of FE calculations showed that the value of triaxiality factor in samples used in the micro-shear test is similar to the value reached in the failure areas of blood chamber.

**D.** In the experiment and numerical model of micro-shear test the critical strain (effective strain) was determined in the TiN nano-coating and it is 0.004 for triaxiality factor  $k = 0.15$ . However, in the macro-model of blood chamber for the same value of triaxiality factor the critical strain is 0.008.

#### Acknowledgements

Financial assistance of the NCN, project no. 2011/01/D/ST8/04087, is acknowledged. The micro-shear tests and TEM's analysis were performed at the WIMiP AGH.

#### REFERENCES

- [1] Y.G. An, H. Vegter, J. Heijne, *J Mater Process Technol.* **209**, 4248-4254 (2009).
- [2] Y. Bai, X. Teng, T. Wierzbicki, *J Eng Mater Technol.* **131**, 1-10 (2009).
- [3] Y. Bai, T. Wierzbicki, *Int J Plast.* **24**, 1071-1096 (2009).
- [4] L. Malcher, F.M. Andrade Pires, J.M.A. Cesar de Sa, *Int J Plast.* **30-31**, 81-115 (2012).
- [5] A. Baldi, L. Francesconi, A. Medda, F. Bertolino, *Exp Mech.* **53**, 1105-1116 (2013).
- [6] J.-K. Heyer, S. Brinckmann, J. Pfetzling-Micklich, G. Eggeler, *Acta Mater.* **62**, 225-238 (2014).
- [7] Y.G. An, H. Vegter, J. Heijne, *J Mater Process Technol.* **209**, 4248-4254 (2009).
- [8] F.F. Wu, W. Zheng, S.D. Wu, Z.F. Zhang, J. Shen, *Acta Mater.* **60**, 2073-2081 (2012).
- [9] Y. Li, M. Luo, J. Gerlach, T. Wierzbicki, *J Mater Process Technol.* **210**, 1858-1869 (2010).
- [10] S. Hao, W.K. Liu, B. Moran, F. Vernerey, G.B. Olson, *Comput Methods Appl Mech Eng.* **193**, 1865-1908 (2004).
- [11] M. Kopernik, A. Milenin, *Arch Civ Mech Eng.* **12**, 178-185 (2012).
- [12] A. Milenin, M. Kopernik, D. Jurkojć, M. Gawlikowski, T. Rusin, M. Darlak, R. Kustosz, *Acta Bioeng Biomech.* **14**, 49-57 (2012).
- [13] G. Konieczny, Z. Opilski, T. Pustelny, M. Gawlikowski, *BioMed Eng.* **11**, 1-13 (2012).
- [14] A. Milenin, M. Kopernik, *Acta Bioeng Biomech.* **13/2**, 13-23 (2011).
- [15] A. Milenin, M. Kopernik, *Acta Bioeng Biomech.* **13/4**, 11-19 (2011).
- [16] M. Kopernik, *Acta Bioeng Biomech.* **15**, 81-87 (2013).
- [17] M. Kopernik, *Arch Metall Mater.* **60**, 127-134 (2015).
- [18] M. Kopernik, A. Milenin, S. Kąc, M. Wróbel, *J Nanomater.* **2014**, 1-12, (2014).
- [19] M. Kopernik, *Adv Eng Mat.* **16**, 1-21 (2014).
- [20] M. Kopernik, A. Milenin, R. Major, J.M. Lackner, *Mater Sci Tech.* **27**, 604-616 (2011).
- [21] J. Kusiński, S. Kąc, Wytwarzanie techniką ablacji laserowej powłok na bazie Ti na podłożu polimerowym, in: R. Kustosz, M. Gonsior, A. Jarosz (Ed.), *Technologie w inżynierii materiałowej i technologiczne metrologiczne dla potrzeb polskich protez serca*, Epigraf Zabrze (2012).
- [22] A. Milenin, *The bases of finite element method*, AGH Uczelniane Wydawnictwa Naukowo-Dydaktyczne, Kraków (2010).
- [23] H. Hirakata, H. Ogiwara, A. Yonezu, K. Minoshima, *Thin Solid Films* **518**, 5249-5256 (2010).